# Energisation Method for Offshore Wind Farms Connected to HVdc via Diode Rectifiers

Oscar Saborío-Romano, *Student Member*, *IEEE*, Ali Bidadfar, *Member*, *IEEE*, Jayachandra N. Sakamuri, Ömer Göksu, Nicolaos A. Cutululis, *Senior Member*, *IEEE*

***Abstract*—Diode rectifiers (DRs) have been recently suggested as a viable alternative for connecting offshore wind farms (OWFs) to HVdc, eliciting growing interest from both industry and academia. However, energisation of DR-connected OWFs is not straightforward. The present study constitutes a proof of concept of a novel energisation method for DR-connected OWFs, in which auxiliary power is provided from the shore through the HVdc link and the dc bus bar of one or more WTs. The proposed method provides an alternative with minimal additional hardware, which can be easily extended to more WTs in the OWF, increasing reliability by providing redundancy. The study includes coinciding auxiliary loads with active and reactive power components and a semi-aggregated OWF model, in which every WT is individually represented in the string containing the energising WT. Two additional sequences of simulation events are considered following the initial energisation sequence. Such sequences comprise wind power taking over the provision of the auxiliary power and the run-up to maximum (available) power production. The simulation results indicate that the proposed method is a suitable alternative for energising OWFs connected to HVdc via DRs.**

***Index Terms*—Diode-rectifier-based HVdc transmission, energisation, grid-forming wind turbine control, offshore wind energy integration**

## I. Introduction

ELECTRICAL infrastructure connecting offshore wind farms (OWFs) to the onshore networks is required to exploit Europe's offshore wind resources further. Thus far, only a few OWFs are connected through HVdc, while the majority export their production via HVac. However, the amount of HVdc-connected OWFs is widely expected to increase, as the associated costs decrease and the distance from shore and size of new OWFs increase [1], [2].

HVdc transmission technology employing voltage source (forced-/self-commutated) converters (VSCs), based on insulated-gate bipolar transistors, has developed significantly since its introduction in 1997. Such technology provides advantages like smaller footprints, fast reversibility of active power flow, independent control of active and reactive power, and the (grid-forming) capability to form ac networks, i.e. to control their ac-side voltage magnitude and frequency. Due to such advantages, the use of VSC-based offshore HVdc terminals has made it possible to develop HVdc-connected OWFs with the prevailing grid-following approach to the control of wind turbines (WTs), in which WTs rely on other (grid-forming) units (e.g. VSC-based offshore HVdc terminals) forming their ac network.

In quest of lowering costs further, (uncontrolled, line-commutated) diode rectifiers (DRs) have been recently suggested as a viable alternative for connecting OWFs to HVdc, eliciting growing interest from both industry and academia [3]–[17]. DR-based offshore HVdc terminals may provide advantages such as even smaller footprints, higher reliability, lower costs and higher efficiency [6], [9]. However, such offshore HVdc terminals lack the grid-forming capability of VSCs, for diodes are passive devices. WTs have consequently been proposed as viable candidates to take over such responsibility, which requires changing their control approach from that of grid-following units to that of grid-forming units [3], [8].

### A. Wind Farm Energisation

WTs and WFs have auxiliary systems (i.e. loads) that need electricity most of the time. Such loads can consist of pitch and yaw motors, navigation lights, oil pumps, air conditioning, dehumidifiers, and measurement, control, protection, communication and safety systems, among others.

When WTs produce electricity, part of the production is used to supply such loads, but auxiliary power must be otherwise provided from local auxiliary energy sources, e.g. batteries or diesel generators, or from the networks connected to them [2]. This is the case when there is no aerodynamic power available from the wind (i.e. the wind speed is below the cut-in wind speed or above the cut-out wind speed of the WTs) or before the WTs are ready to produce power.

The use of VSC-based offshore HVdc terminals allows remote OWFs to draw the auxiliary power required in such cases from the HVdc networks connected to them. This, however, is not possible for OWFs connected to HVdc via DRs, as power through the DRs can only flow towards the shore. As a consequence, such OWFs must be energised by other means. This is also the case for OWFs connected to HVdc networks via VSCs, when such offshore converters are not operational [2], [18]–[20].

Different solutions have been proposed for energising OWFs connected to HVdc via DRs [5], [7], [10]. The use of local auxiliary energy sources or the connection to neighbouring energised offshore ac networks, e.g. other OWFs, have been proposed in [7]. The latter has been considered in several subsequent studies [12].

This work has received funding from the European Union's Horizon 2020 research and innovation programme under grant agreement No 691714.

O. Saborío-Romano, A. Bidadfar, Ö. Göksu and N. A. Cutululis are with the Department of Wind Energy, Technical University of Denmark, Frederiksborgvej 399, 4000 Roskilde, Denmark (e-mail: osro@dtu.dk; abid@dtu.dk; omeg@dtu.dk; niac@dtu.dk).

J. N. Sakamuri is with Vattenfall, Jupitervej 6, 6000 Kolding, Denmark (e-mail: jayachandranaidu.sakamuri@vattenfall.com).

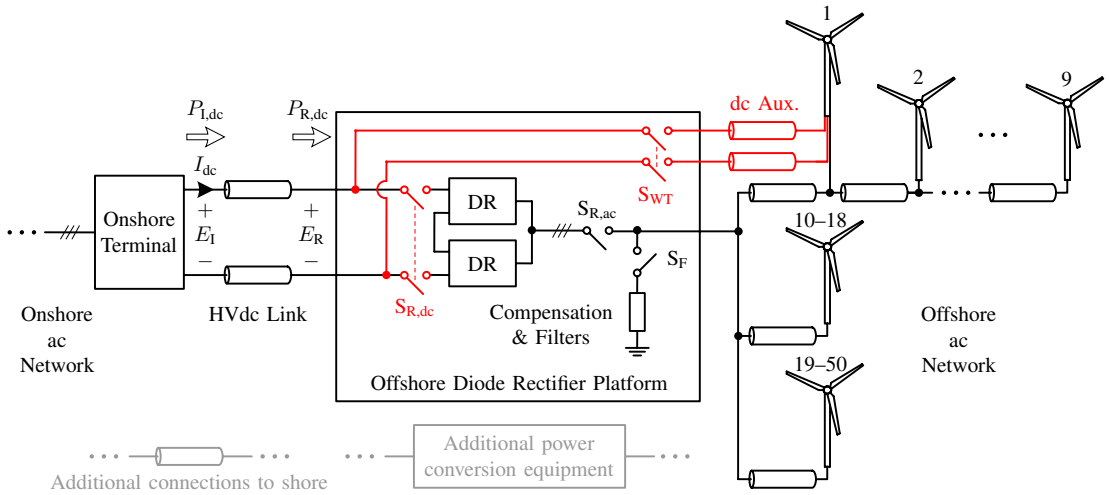


Fig. 1. Overview of the studied system; red: additional equipment introduced by the proposed energisation method, grey: alternatives in literature for providing the auxiliary power from onshore ac networks

Solutions for providing the auxiliary power from onshore ac networks are represented in grey in Fig. 1. Some of these rely on additional long submarine cables connecting the onshore ac networks and the OWFs. The use of additional LVdc links has been proposed in [7], which requires additional VSC-based power conversion terminals. Moreover, additional MVac *umbilical* cables interconnecting the onshore and offshore ac networks have been introduced in [7]–[10]. Such umbilical cables have been considered in several subsequent studies [11]–[15], [17], and have been assumed to be disconnected during normal operation, i.e. their use has been restricted to the energisation of the corresponding OWFs. Other solutions avoid the need for additional long submarine cables by introducing additional power conversion equipment offshore to effectively bypass the DRs during energisation [5], [7].

In pursuit of increasing reliability and lowering costs and environmental impact, a new energisation method has been proposed in [21] for the case of an OWF connected to an onshore ac network through an HVdc link having a DR-based offshore terminal and a full-bridge-VSC-based onshore terminal. During energisation, auxiliary power is provided from the shore through the HVdc link and the dc bus bar of one or more WTs. The method only requires short additional dc cables connecting the dc bus bar of such *energising* WT to the HVdc link, and corresponding dc disconnectors at the cable terminals and at the dc terminals of the DR platform, highlighted in red in Figs. 1 and 2.

This work extends the assessment in [21] to include coinciding auxiliary loads with active and reactive power components and a a semi-aggregated OWF model, in which every WT in the string containing the energising WT is individually represented. Two additional sequences of simulation events are considered following the initial sequence, in which the OWF is energised with the proposed method. In the second sequence, wind power takes over the provision of the auxiliary power, once enough aerodynamic power becomes available from the wind. The last sequence comprises the transmission network start-up and the ramp-up of production to maximum (available) power, once the aerodynamic power available from the wind is greater than the minimum production limit [12].

The rest of the paper is organised as follows. The studied system and the main control algorithms are described in Section II. In Section III, the considered sequences of events are described, and corresponding simulation results are presented and discussed. Finally, concluding remarks are made in Section IV.

## II. Modelling and Control

Fig. 1 shows an overview of the studied system. The system is based on that described in [12], [13] and consists of one of three $400\,\mathrm{MW}$ OWFs connected to an onshore ac network by means of a $200\,\mathrm{km}$ long $1200\,\mathrm{MW}$ $\pm 320\,\mathrm{kV}$ monopolar HVdc link and corresponding onshore HVdc terminal, operating at a third of the rated voltage (i.e. the nominal voltage is approximately $213\,\mathrm{kV}$, and the nominal power is $400\,\mathrm{MW}$). Balanced/symmetric operation is assumed. The offshore HVdc terminal: one of three diode rectifier platforms (one per OWF), depicted in Fig. 1, consists of two (uncontrolled, line-commutated) diode-based 12-pulse rectifiers (DRs) connected in series, with corresponding reactive power compensation and filter bank on their ac side.

The OWF has 50 type-4 (full-converter) $8\,\mathrm{MW}$ WTs, laid out in 6 strings. The WT converter nominal ac voltage is $3.3\,\mathrm{kV}$. The first string, comprised of WTs 1–9 is represented in detail. The second string, consisting of WTs 10–18, is aggregated into an equivalent $72\,\mathrm{MW}$ WT and corresponding cable equivalent $\pi$ circuit using the method proposed in [22]. Likewise, the other 4 strings, comprising WTs 19–50, are aggregated into an equivalent $256\,\mathrm{MW}$ WT and corresponding cable equivalent $\pi$ circuit.

The front-end (line-side) network of the $k$th wind turbine(s), $\mathrm{WT}_k$, is shown in Fig. 2. The coinciding auxiliary loads are represented within each (equivalent) WT by a constant power load, with an active power component, $P_{\mathrm{a},k}$, corresponding to $0.2\,\%$ of the nominal power ($800\,\mathrm{kW}$ in total for the whole $400\,\mathrm{MW}$ WF) and a power factor of $0.83$, i.e. a reactive power

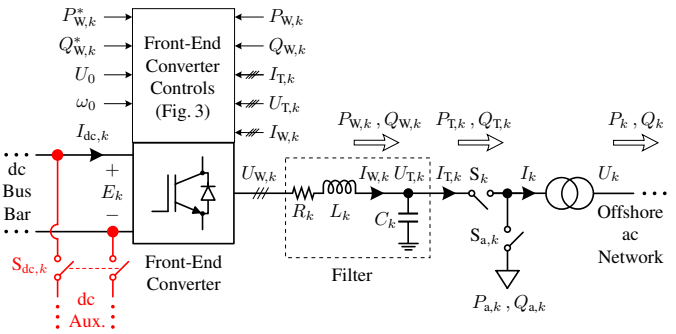


Fig. 2. Front-end (line-side) network of the $k$th wind turbine(s); red: additional equipment introduced in the *energising* wind turbine(s) by the proposed energisation method

component, $Q_{\mathrm{a},k}$, corresponding to $0.134\,\%$ of the nominal power ($536\,\mathrm{kVAr}$ in total for the whole $400\,\mathrm{MW}$ WF).

$\mathrm{WT}_1$ is chosen as the energising WT: its dc auxiliary supply terminal can be connected to that of the DR platform by means of additional dc auxiliary cables. Additional dc disconnectors are also introduced at the corresponding terminals, $\mathrm{S}_{\mathrm{dc},1}$, $\mathrm{S}_{\mathrm{WT}}$, and at the dc terminals of the DR platform, $\mathrm{S}_{\mathrm{R,dc}}$. The additional equipment introduced by the method is shown in Figs. 1 and 2, highlighted in red. The HVdc link dynamics are assumed to dominate in the energisation path. The influence of the other elements, e.g, dc auxiliary cables, effectively interconnecting the HVdc link and the dc bus bar of $\mathrm{WT}_1$ (when $\mathrm{S}_{\mathrm{WT}}$ is closed) is thus neglected, i.e. the voltage at the dc bus bar of $\mathrm{WT}_1$, $E_1$, is approximately equal to the voltage at the offshore terminal of the HVdc link, $E_{\mathrm{R}}$, during energisation.

WT rotor and back-end (generator-side) network dynamics are not considered, as they are not relevant to the case in question. Pulse-width modulation (PWM) is assumed to be done in the linear range, switching effects and any delay due to the implementation of the PWM are neglected, and average value models are used to represent the WT FECs. Focus is given to dynamics not faster than the WT FEC (inner/lower) current control loops, which are designed to have a bandwidth of $200\,\mathrm{Hz}$.

### A. Wind Turbine Front-End Converter Controls

The grid-forming WT FEC controls, shown in Fig. 3, are based on those proposed in [16] and are implemented on a rotating reference frame (RRF) with angular speed given by $\omega_k$, oriented on the voltage at the filter capacitor, $U_{\mathrm{T},k}$, and with the quadrature (q) axis leading the direct (d) axis by $90°$.

In each WT front-end network, the filter capacitor voltage direct (d) and quadrature (q) axis components are regulated by the FEC lower/inner control loops to follow the corresponding references, $U^*_{\mathrm{Td},k}, U^*_{\mathrm{Tq},k}$, respectively. $U^*_{\mathrm{Td},k}$ consists of two components: the offshore ac network voltage set point, $U_0$, common to all WTs, and a component individual to each WT, which is altered to control the FEC active power output, $P_{\mathrm{W},k}$. In an additional control loop based on the FEC phase-locked loop (PLL), a proportional regulator manipulates $U^*_{\mathrm{Tq},k}$ to control $\omega_k$. The reference to such additional loop also consists of two components: the offshore ac network (angular) frequency set point, $\omega_0$, common to all WTs, and a component individual to each WT, which is altered to control the FEC reactive power output, $Q_{\mathrm{W},k}$.

When the WF is exporting power, the FEC upper/outer control loops in each WT regulate $P_{\mathrm{W},k}$ and $Q_{\mathrm{W},k}$ as follows. A proportional-integral (PI) regulator controls $P_{\mathrm{W},k}$ to follow the corresponding reference, $P^*_{\mathrm{W},k}$, whereas $Q_{\mathrm{W},k}$ is controlled by a proportional regulator (reactive-power-frequency droop) with a given reference, $Q^*_{\mathrm{W},k}$, so that reactive power is shared among WT FECs (avoiding overcurrents and reactive current circulation). Values for the control parameters and limits are given in Table II.

## III. Simulation Results

Results of the dynamic simulations performed in PSCAD are shown in Figs. 4–6. All (equivalent) WT front-end networks and corresponding converter controls have the same parameter per-unit (pu) values. Moreover, $\omega_0 = 1\,\mathrm{pu}$ for all of them. Quantities related to the HVdc link are depicted in Subfigs. (a)–(c). Subfigs. (a) illustrate the voltage at the onshore and offshore ends of the HVdc link, $E_{\mathrm{I}}$ and $E_{\mathrm{R}}$, respectively, while the HVdc link current, $I_{\mathrm{dc}}$, is portrayed in Subfigs. (b). Likewise, the active power flowing out of the onshore terminal. $P_{\mathrm{I,dc}}$, and into the offshore diode rectifier platform, $P_{\mathrm{R,dc}}$, are illustrated shown in Subfigs. (c).

The remaining subfigs. (d)–(h) depict quantities related to the offshore ac network. The offshore ac network (angular) frequency, $\omega$, is portrayed in Subfigs. (d), whereas the WT terminal rms voltages, $U_k$, and output rms currents, $I_k$, are presented in Subfigs. (e) and (f), respectively. Finally, the WT active and reactive power output, $P_k$ and $Q_k$, respectively, are shown in Subfigs. (g) and (h), respectively.

Table I summarises the simulation events, which are discussed in the following. The events are grouped in stages to facilitate discussion. Three consecutive sequences of events have been considered. Sequence 1, depicted in Fig. 4, corresponds to the energisation of the OWF with the proposed method. In Sequence 2, portrayed in Fig. 5, wind power takes over the provision of the auxiliary power, once enough aerodynamic power becomes available from the wind. Lastly, Sequence 3, illustrated in Fig. 6, comprises the transmission network start-up and the ramp-up of production to maximum (available) power, once the aerodynamic power available from the wind is greater than the minimum production limit [12].

### A. Stage 0: Initial Conditions

Initially, the aerodynamic power available from the wind is assumed to be 0, i.e. the wind speed is assumed to be below the cut-in wind speed or above the cut-out wind speed of the WTs. The WTs, offshore ac network and HVdc link are de-energised, the voltage and WT active/reactive power set points, $E^*_{\mathrm{R}}, U_0, P^*_{\mathrm{W},k}, Q^*_{\mathrm{W},k}$, are set to 0, and all ac circuit breakers and dc disconnectors, shown in Figs. 1 and 2, are open. The regulators in the WT FEC PLL and frequency and active/reactive power controls are disabled for all WTs. In this way, $\omega_k = \omega_0$, $U^*_{\mathrm{Td}} = U_0$, $U^*_{\mathrm{Tq}} = 0$ and the WT FEC controls are equivalent to those used in [21].

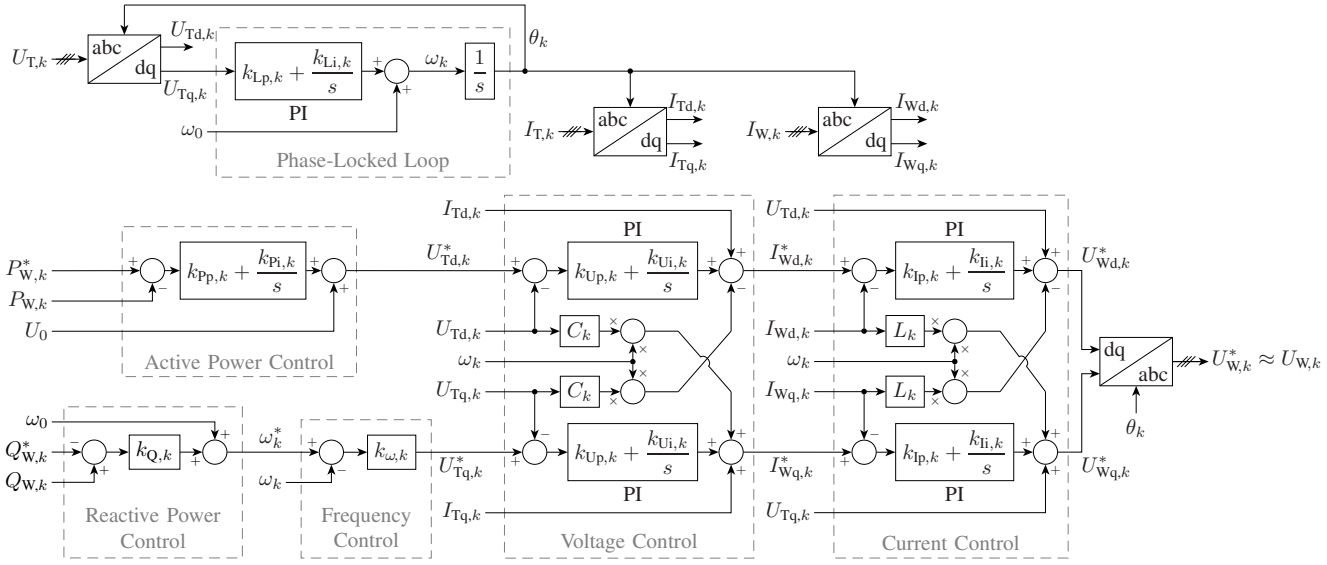


Fig. 3. Front-end (line-side) converter controls of the $k$th wind turbine(s); parameter values and limits given in Table II

### B. Stage 1: $WT_1$ dc Bus Bar Energisation

At $t = 0\,\mathrm{s}$, the dc disconnectors $S_{WT}$ and $S_{dc,1}$ are closed, so that the dc auxiliary supply effectively connects the dc bus bar of $WT_1$ to the HVdc link, $E_1 \approx E_R$. Between $t = 1\,\mathrm{s}$ and $t = 6.39\,\mathrm{s}$, the onshore terminal energises the HVdc link and the dc bus bar of $WT_1$ as the direct voltage set point, $E_R^*$, is increased from 0 to the WT dc bus bar nominal voltage (approximately $5.39\,\mathrm{kV}$), as illustrated in Subfig. 4a.

### C. Stage 2: Offshore ac Network Energisation

$WT_1$ main ac circuit breaker, $S_1$, is closed at $t = 9\,\mathrm{s}$, and the corresponding FEC then energises the offshore ac network, establishing its voltage and frequency, as the offshore ac network voltage set point, $U_0$, is increased from 0 to $0.9\,\mathrm{pu}$ between $t = 10\,\mathrm{s}$ and $t = 11\,\mathrm{s}$, as shown in Subfigs. 4d and 4e. In doing so, it draws about $339\,\mathrm{kW}$ from the onshore terminal, as illustrated in Subfig. 4c, to supply the no-load losses. The onshore terminal controller calculates the voltage drop in the HVdc link using the measured $I_{dc}$ and estimated HVdc link resistance, $\tilde{R}_{dc}$, and compensates for it by increasing $E_I$ accordingly, maintaining $E_R$ close to its reference value, as shown in Subfigs. 4a and 4b. Inrush currents are avoided by energising all WT transformers at the same time with the voltage ramp. If, however, a WT is disconnected and needs to be re-energised by the established offshore ac network, proven solutions such as pre-insertion resistors and point on wave switching can be employed to reduce such currents.

### D. Stage 3: Auxiliary Load Energisation

At $t = 15\,\mathrm{s}$, ac circuit breakers $S_{a,k}$ are closed, and the auxiliary loads are energised, as depicted most notably in Subfigs. 4c and 4g. As portrayed in Subfig. 4f, less than half of the WT nominal rms current is needed to energise the studied OWF with the proposed method. Furthermore, it requires an HVdc link current of less than $170\,\mathrm{A}$, i.e. less than $10\,\%$ of its nominal current, as shown in Subfig. 4b, leaving enough HVdc link current capacity to energise the other two $400\,\mathrm{MW}$ OWFs in the same way. In the studied system, such current constitutes the necessary capacity of the dc auxiliary supply cables, introduced in the proposed energisation method. Such capacity can in turn determine the current limit for the corresponding protections.

### E. Stage 4: Connection of FECs from WTs 2–50

Once enough aerodynamic power becomes available from the wind and the WTs start up, the regulators in the FEC PLL and frequency and reactive power control loops are enabled at $t = 20.1\,\mathrm{s}$ for WTs 2–50, as are also the proportional terms of the regulators in the corresponding active power control loops. The main ac circuit breaker of $WT_2$, $S_2$ is then closed at $t = 20.5\,\mathrm{s}$, so that the FEC from $WT_2$ is connected to the offshore ac network, as illustrated by Subfig. 5f. At $t = 21\,\mathrm{s}$, the regulators in the FEC PLL and frequency and reactive power control loops are enabled for $WT_1$, so that all connected WT FECs contribute autonomously to regulating the offshore ac network voltage magnitude and frequency, while sharing the reactive power consumption/production, as portrayed in Subfigs. 5d, 5e and 5h. The main ac circuit breakers, $S_k$, are then closed at $0.5\,\mathrm{s}$ intervals for the remaining WTs 3–50, between $t = 21.5\,\mathrm{s}$ and $t = 25.5\,\mathrm{s}$, so that the corresponding WT FECs are connected to the offshore ac network, as depicted in Subfigs. 5f and 5h. Each WT FEC synchronises automatically with the offshore ac network as it is connected.

### F. Stage 5: $WT_1$ FEC Disconnection

At $t = 26\,\mathrm{s}$, the proportional term of the regulator in the $WT_1$ FEC active power control loop is enabled, so that all connected WT FECs share the active power production, as shown in Subfig. 5g. The $WT_1$ FEC is then disconnected from the offshore ac network at $t = 26.5\,\mathrm{s}$ by opening $S_1$, as illustrated most notably by Subfigs. 5f and 5g. From this moment forth, all auxiliary power is provided from the wind.

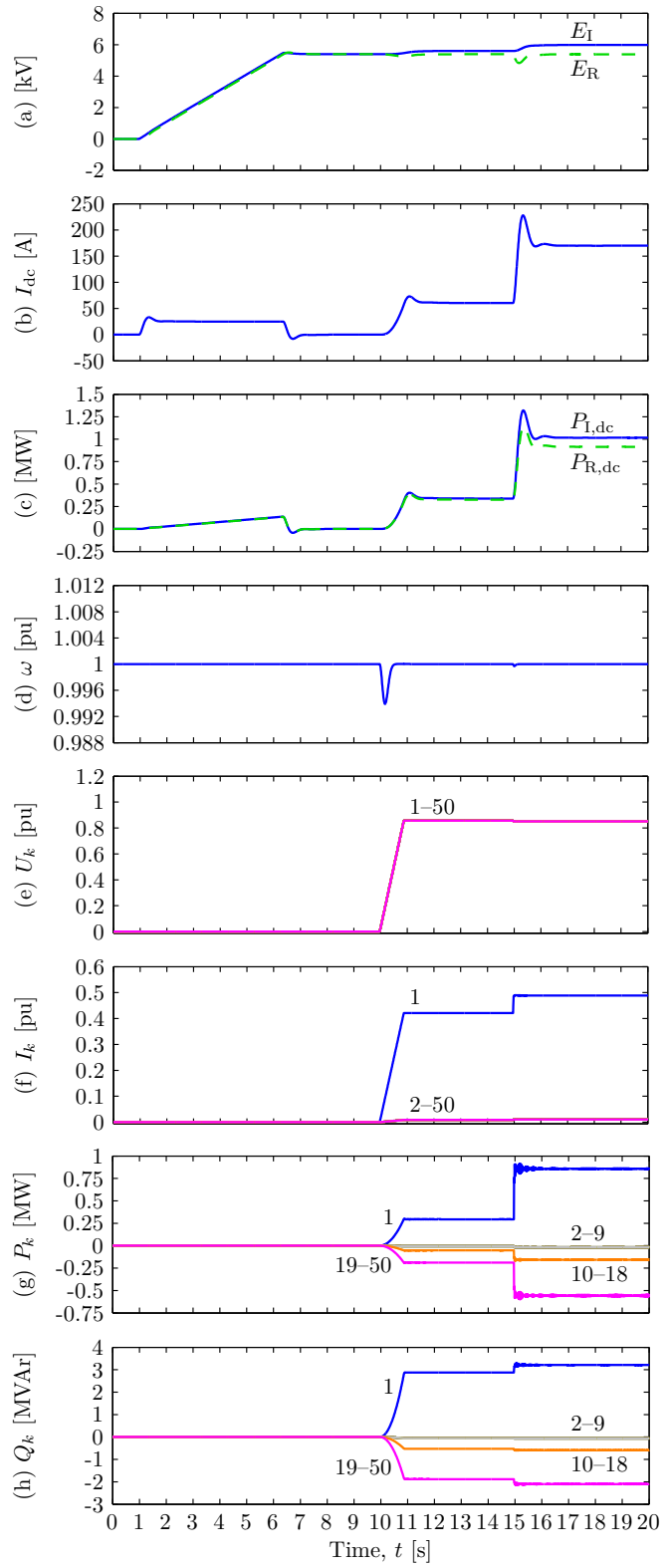


Fig. 4. Simulation results for Sequence 1: (a) voltage at the onshore and offshore ends of the HVdc link, $E_{\mathrm{I}}$ and $E_{\mathrm{R}}$, respectively; (b) HVdc link current; (c) active power flowing out of the onshore terminal, $P_{\mathrm{I,dc}}$, and into the offshore diode rectifier platform, $P_{\mathrm{R,dc}}$; (d) offshore ac network (angular) frequency; (e) WT$_k$ terminal rms voltage; (f) WT$_k$ output rms current; (g) WT$_k$ active power output; (h) WT$_k$ reactive power output; values of $k$ indicated next to each visible trace within each subfig.

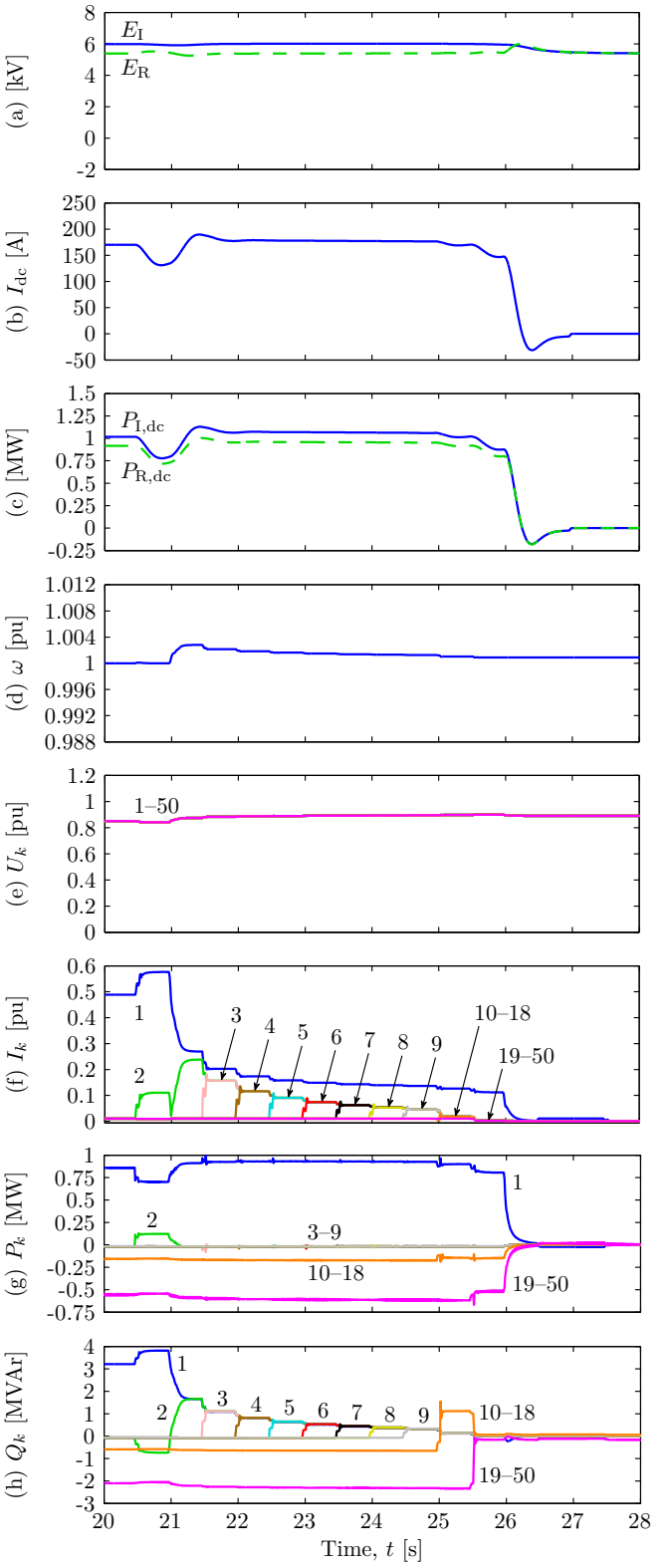


Fig. 5. Simulation results for Sequence 2: (a) voltage at the onshore and offshore ends of the HVdc link, $E_{\mathrm{I}}$ and $E_{\mathrm{R}}$, respectively; (b) HVdc link current; (c) active power flowing out of the onshore terminal, $P_{\mathrm{I,dc}}$, and into the offshore diode rectifier platform, $P_{\mathrm{R,dc}}$; (d) offshore ac network (angular) frequency; (e) WT$_k$ terminal rms voltage; (f) WT$_k$ output rms current; (g) WT$_k$ active power output; (h) WT$_k$ reactive power output; values of $k$ indicated next to each visible trace within each subfig.

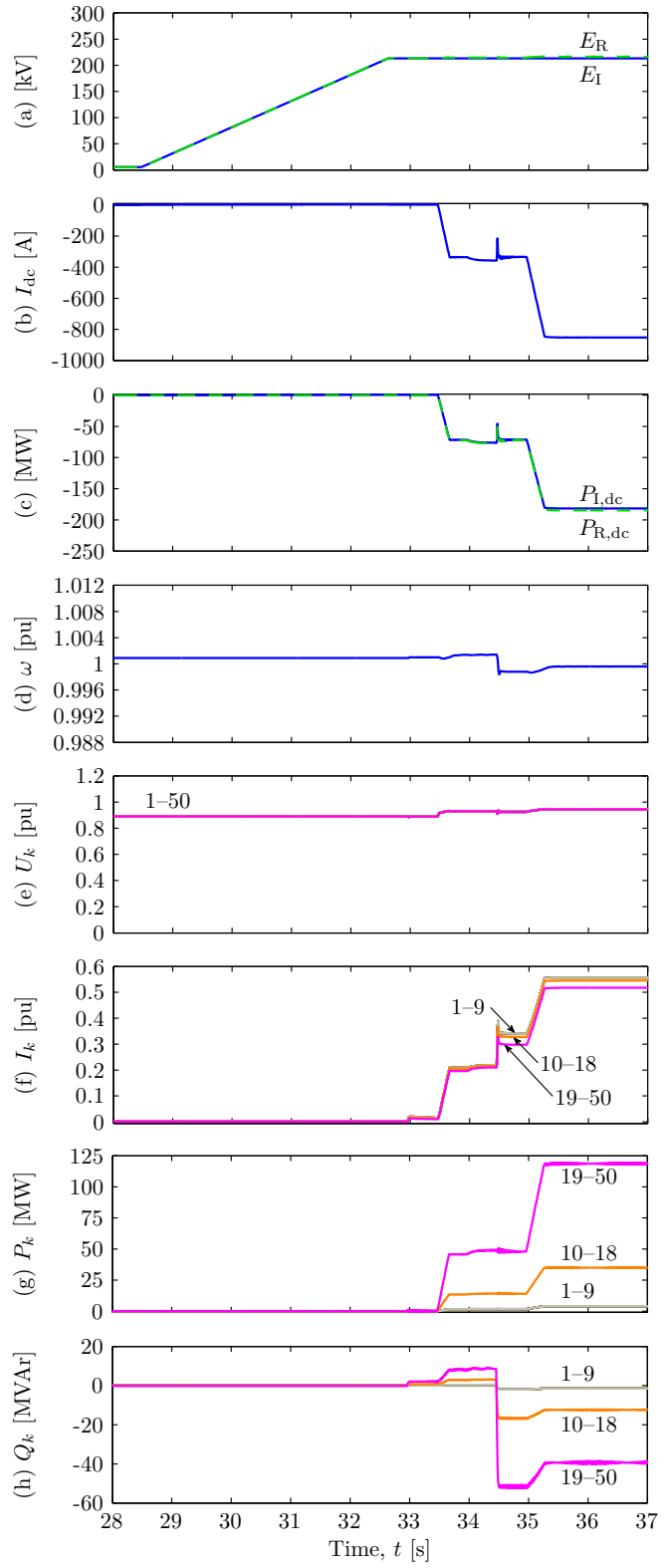


Fig. 6. Simulation results for Sequence 3: (a) voltage at the onshore and offshore ends of the HVdc link, $E_I$ and $E_R$, respectively; (b) HVdc link current; (c) active power flowing out of the onshore terminal, $P_{I,dc}$, and into the offshore diode rectifier platform, $P_{R,dc}$; (d) offshore ac network (angular) frequency; (e) $WT_k$ terminal rms voltage; (f) $WT_k$ output rms current; (g) $WT_k$ active power output; (h) $WT_k$ reactive power output; values of $k$ indicated next to each visible trace within each subfig.

TABLE I
SIMULATION EVENTS

| Stage | Time [s] | Events |
|---|---|---|
| 0 | $< 0$ | No power available from the wind; WTs, offshore ac network and HVdc link de-energised; $E_R^*$, $U_0$, $P_{W,k}^*$ and $Q_{W,k}^*$ set to 0; all ac circuit breakers and dc disconnectors open; FEC PLL and frequency and (active/reactive) power controls disabled for all WTs |
| **Sequence 1: Energisation from Shore** (Fig. 4) | | |
| 1 | 0 | $S_{WT}$ and $S_{dc,1}$ closed: dc auxiliary supply effectively connects the dc bus bar of $WT_1$ to the HVdc link |
| | $1 - 6.39$ | $E_R^*$ increased from 0 to 5.39 kV; onshore terminal energises the HVdc link and the dc bus bar of $WT_1$ |
| 2 | 9 | $S_1$ closed: $WT_1$ FEC connected to the ac network |
| | $10 - 11$ | $U_0$ increased from 0 to 0.9 pu: $WT_1$ energises the offshore ac network, establishing its voltage and frequency; all auxiliary power is provided from shore |
| 3 | 15 | $S_{a,k}$ closed: auxiliary loads energised |
| **Sequence 2: Wind Power Takes Over** (Fig. 5) | | |
| 4 | 20 | Enough aerodynamic power available from the wind |
| | 20.1 | FEC PLL and frequency and reactive power controls enabled for WTs 2–50; FEC active power proportional control enabled for WTs 2–50 |
| | 20.5 | $S_2$ closed: $WT_2$ FEC connected to the ac network |
| | 21 | $WT_1$ FEC PLL and frequency and reactive power controls enabled; connected WT FECs regulate ac network voltage magnitude and frequency, while sharing the reactive power consumption/production |
| | $21.5 - 25.5$ | $S_k$ closed at 0.5 s intervals for WTs 3–50: FECs from WTs 3–50 connected to the ac network |
| 5 | 26 | $WT_1$ FEC active power proportional control enabled; connected FECs share the active power production |
| | 26.5 | $S_1$ open: $WT_1$ FEC disconnected from the ac network; all auxiliary power is provided from the wind |
| 6 | 27 | $S_{WT}$ and $S_{dc,1}$ open: dc auxiliary supply disconnected; $WT_1$ BEC takes over control of $E_1$ |
| | 27.5 | $S_1$ closed: $WT_1$ FEC reconnected to the ac network |
| **Sequence 3: Wind Farm Begins Exporting Power** (Fig. 6) | | |
| 7 | 28.1 | $S_{R,dc}$ closed: DRs connected to the HVdc link |
| | $28.5 - 32.6$ | $E_R^*$ increased from 5.39 kV to 213 kV |
| | 33 | Aerodynamic power available from the wind greater than minimum production limit; $S_{R,ac}$ closed: DRs connected to and energised from the ac network; the WF can begin exporting power |
| 8 | $33.5 - 33.7$ | $P_{W,k}^*$ increased from 0 to 0.2 pu: the WF begins exporting power |
| | 34 | FEC active power integral control enabled for all WTs |
| | 34.5 | $S_F$ closed: reactive power compensation and filter bank connected |
| | $35 - 35.3$ | $P_{W,k}^*$ increased from 0.2 pu to 0.5 pu: the WF increases its production to maximum (available) power |

### G. Stage 6: $WT_1$ FEC Reconnection

The dc auxiliary supply is disconnected at $t = 27\,\mathrm{s}$ by opening $S_{WT}$ and $S_{dc,1}$, as portrayed in Subfig. 5b, and the back-end converter (BEC) of $WT_1$ takes over the control of the WT dc bus bar voltage, $E_1$. At $t = 27.5\,\mathrm{s}$, the $WT_1$ FEC is reconnected to the offshore ac network by closing $S_1$, as depicted most notably by Subfigs. 5f and 5g.

### H. Stage 7: Transmission Network Start-up

At $t = 28.1\,\mathrm{s}$, the DRs are connected to the HVdc link by closing the corresponding dc disconnectors, $S_{R,dc}$. The onshore terminal then increases the HVdc link voltage to its nominal value as $E_R^*$ is increased from $5.39\,\mathrm{kV}$ to $213\,\mathrm{kV}$ between $t = 28.5\,\mathrm{s}$ and $t = 32.6\,\mathrm{s}$, as shown in Subfig. 6a. Once the aerodynamic power available from the wind is greater than the minimum production limit [12], the DRs are connected to and energised from the offshore ac network by closing the corresponding ac circuit breakers, $S_{R,ac}$ at $t = 33\,\mathrm{s}$. Proven solutions such as pre-insertion resistors and point on wave switching can be employed to reduce any inrush current resulting from the energisation of the DR transformers. From this moment forth, the WF can begin exporting power.

### I. Stage 8: WF Power Production Ramp-up

$P_k^*$ is increased from 0 to $0.2\,\mathrm{pu}$ between $t = 33.5\,\mathrm{s}$ and $t = 33.7\,\mathrm{s}$, and the WF begins exporting power, as illustrated in Subfigs. 6c and 6g. At $t = 34\,\mathrm{s}$, the integral terms of the regulators in WT FEC active power control loops are enabled. The reactive power compensation and filter bank are then connected at $t = 34.5\,\mathrm{s}$, as portrayed in Subfig. 6h. Finally, the WF increases its production to maximum (available) power as $P_k^*$ is increased from $0.2\,\mathrm{pu}$ to $0.5\,\mathrm{pu}$ between $t = 35\,\mathrm{s}$ and $t = 35.3\,\mathrm{s}$, as depicted in Subfigs. 6c and 6g.

### J. Further Comments

The proposed energisation method relies on accurate and independent control of the reduced voltage in the dc transmission network. This may require the use of, for example, a full-bridge modular multilevel converter and an additional set of measurement devices onshore. Likewise, additional protections (settings) may be required. Even though reliability requirements may not allow OWFs to do without local auxiliary energy sources, the method can certainly help reduce the reliance on such energy sources. Moreover, the applicability of the method to WTs with LV power converters will depend on the amount of auxiliary power to be transmitted through the HVdc cables and the thermal limits of such cables. Further research is needed to asses the applicability of the proposed energisation method and of DR connection technology in general to multiterminal HVdc networks.

## IV. Conclusions

The simulation results indicate that the proposed method is a suitable alternative for energising OWFs connected to HVdc via DRs. Using MV WT converters, the necessary auxiliary power can be provided to the studied OWF through the dc bus bar of the *energising* WT, while leaving enough HVdc link current capacity to energise the other OWFs in the same way. The method provides a robust and reliable alternative with minimal additional hardware: short dc cables connecting the dc bus bar of the energising WT to the HVdc link, and dc disconnectors at the terminals of such cables and at the DR dc terminals. This can be easily extended to more WTs in the OWF, increasing reliability by providing redundancy.

Once enough aerodynamic power becomes available from the wind and the WTs start up, wind power can take over the provision of the auxiliary power, and the dc auxiliary supply can be disconnected. With the considered grid-forming WT FEC controls, each FEC synchronises automatically with the offshore ac network as it is connected, and all connected FECs contribute autonomously to regulating the offshore ac network voltage magnitude and frequency, while sharing the active power production and the reactive power consumption/ production. The WF can then begin exporting power, as soon as the transmission network is ready and the aerodynamic power available from the wind surpasses the minimum production limit.

## Appendix

TABLE II
$WT_k$ FRONT-END CONVERTER CONTROL PARAMETERS AND LIMITS

| Par. | Value | Par. | Value | Par. | Value |
|---|---|---|---|---|---|
| $C_k$ | $0.05\,\mathrm{pu}$ | $k_{\mathrm{Lp},k}$ | $0.16\,\mathrm{pu}$ | $k_{\mathrm{Q},k}$ | $0.01\,\mathrm{pu}$ |
| $k_{\mathrm{Ii},k}$ | $0.04\,\mathrm{pu/s}$ | $k_{\omega,k}$ | $50\,\mathrm{pu}$ | $k_{\mathrm{Ui},k}$ | $40\,\mathrm{pu/s}$ |
| $k_{\mathrm{Ip},k}$ | $0.4\,\mathrm{pu}$ | $k_{\mathrm{Pi},k}$ | $40\,\mathrm{pu/s}$ | $k_{\mathrm{Up},k}$ | $4\,\mathrm{pu}$ |
| $k_{\mathrm{Li},k}$ | $1.6 \times 10^{-4}\,\mathrm{pu/s}$ | $k_{\mathrm{Pp},k}$ | $4\,\mathrm{pu}$ | $L_k$ | $0.1\,\mathrm{pu}$ |
| **Limits**: | $0 \leq I^*_{\mathrm{W},k} \leq 1.1\,\mathrm{pu}$ | , | $0 \leq U^*_{\mathrm{W},k} \leq 1.1\,\mathrm{pu}$ | | |

## Acknowledgement

The authors gratefully acknowledge the contributions of Lorenzo Zeni and Poul E. Sørensen to the discussions leading up to this work.

## References

[1] E. Prieto-Araujo, F. D. Bianchi, A. Junyent-Ferré, and O. Gomis-Bellmunt, "Methodology for Droop Control Dynamic Analysis of Multiterminal VSC-HVDC Grids for Offshore Wind Farms," *IEEE Transactions on Power Delivery*, vol. 26, no. 4, pp. 2476–2485, Oct. 2011.

[2] CIGRÉ Working Group B3.36, "Special Considerations for AC Collector Systems and Substations Associated with HVDC-Connected Wind Power Plants," Paris, France, Technical Brochure 612, Mar. 2015.

[3] R. M. Blasco-Giménez, S. C. Añó-Villalba, J. Rodríguez-D'Derlée, F. Morant-Anglada, and S. I. Bernal-Pérez, "Distributed Voltage and Frequency Control of Offshore Wind Farms Connected With a Diode-Based HVdc Link," *IEEE Transactions on Power Electronics*, vol. 25, no. 12, pp. 3095–3105, Dec. 2010.

[4] R. M. Blasco-Giménez, S. C. Añó-Villalba, J. Rodríguez-D'Derlée, S. I. Bernal-Pérez, and F. Morant-Anglada, "Diode-Based HVdc Link for the Connection of Large Offshore Wind Farms," *IEEE Transactions on Energy Conversion*, vol. 26, no. 2, pp. 615–626, Mar. 2011.

[5] E. V. Larsen, "Electric power transmission system for wind turbine and wind turbine farm and method for operating same," United States Patent Application Publication US 2011/0140511 Al, 16th Jun. 2011.

[6] S. I. Bernal-Pérez, S. C. Añó-Villalba, R. M. Blasco-Giménez, and J. Rodríguez-D'Derlée, "Efficiency and Fault Ride-Through Performance of a Diode-Rectifier- and VSC-Inverter-Based HVDC Link for Offshore Wind Farms," *IEEE Transactions on Industrial Electronics*, vol. 60, no. 6, pp. 2401–2409, Jun. 2013.

[7] H. J. Knaak, P. Menke, T. Schröck, R. Schuster, and T. Westerweller, "Wind farm connection having a diode rectifier," International Patent Application Publication WO 2014/131454 A1, 4th Sep. 2014.

[8] T. Christ, S. Seman, and R. Zurowski, "Investigation of DC Converter Nonlinear Interaction with Offshore Wind Power Park System," in *Proceedings of the 2015 EWEA Offshore Conference*, Copenhagen, Denmark, 10th–12th Mar. 2015.

[9] P. Menke, R. Zurowski, T. Christ, S. Seman, G. Giering, T. Hammer, W. Zink, F. Hacker, D. Imamovic, J. Thisted, P. Brogan, and N. Goldenbaum, "2nd Generation DC Grid Access for Large Scale Offshore Wind Farms," in *Proceedings of the 14th Wind Integration Workshop*, Brussels, Belgium, 20th–22nd Oct. 2015.

[10] J. Dorn, D. Ergin, T. Hammer, H. J. Knaak, P. Menke, J. Møller, R. Schuster, H. Stiesdal, and J. Thisted, "Converter station with diode rectifier," United States Patent Application Publication US 2016/0013653 Al, 14th Jan. 2016.

[11] C. Prignitz, H. G. Eckel, S. Achenbach, F. Augsburger, and A. Schön, "FixReF: A control strategy for offshore wind farms with different wind turbine types and diode rectifier HVDC transmission," in *Proceedings of the IEEE 7th International Symposium on Power Electronics for Distributed Generation Systems (PEDG 2016)*, Vancouver, BC, Canada, 27th–30th Jun. 2016.

[12] PROMOTioN, "Deliverable 3.1: Detailed functional requirements to WPPs," Project Deliverable, Dec. 2016. [Online]. Available: https://www.promotion-offshore.net/fileadmin/PDFs/D3.1_PROMOTioN_Deliverable_3.1_Detailed_functional_requirements_to_WPPs.pdf.

[13] ——, "Deliverable 3.2: Specifications of the control strategies and the simulation test cases," Project Deliverable, Mar. 2017. [Online]. Available: https://www.promotion-offshore.net/fileadmin/PDFs/D3.2_Specifications_Control_strategies_and_simulation_test_cases.pdf.

[14] C. Neumann, H.-G. Eckel, S. Achenbach, and F. Augsburger, "Auxiliary Power Supply in a FixReF Controlled Offshore Wind Power Plant with Diode Rectifier HVDC Transmission," in *Proceedings of the 16th Wind Integration Workshop*, Berlin, Germany, 25th–27th Oct. 2017.

[15] PROMOTioN, "Deliverable 3.4: Results on control strategies of WPPs connected to DR-HVDC," Project Deliverable, Jan. 2018. [Online]. Available: https://www.promotion-offshore.net/fileadmin/PDFs/D3.4_PROMOTioN_Results_on_control_strategies_of_WPPs_connected_to_DR-HVDC.pdf.

[16] L. Yu, R. Li, and L. Xu, "Distributed PLL-Based Control of Offshore Wind Turbines Connected With Diode-Rectifier-Based HVDC Systems," *IEEE Transactions on Power Delivery*, vol. 33, no. 3, pp. 1328–1336, Jun. 2018.

[17] R. Ramachandran, S. Poullain, A. Benchaib, S. Bacha, and B. Francois, "AC Grid Forming by Coordinated Control of Offshore Wind Farm connected to Diode Rectifier based HVDC Link – Review and Assessment of Solutions," in *Proceedings of the 20th European Conference on Power Electronics and Applications (EPE 2018 – ECCE Europe)*, Riga, Latvia, 17th–21st Sep. 2018.

[18] I. Arana-Aristi, A. Hernández, G. H. Thumm, and J. Holbøll, "Energization of Wind turbine Transformers With an Auxiliary Generator in a Large Offshore Wind Farm During Islanded Operation," *IEEE Transactions on Power Delivery*, vol. 26, no. 4, pp. 2792–2800, Oct. 2011.

[19] J. Berggren, "Study of auxiliary power systems for offshore wind turbines: An extended analysis of a diesel gen-set solution," Master's thesis, Uppsala University, Uppsala, Sweden, Jun. 2013.

[20] L. Cai, U. Karaagac, and J. Mahseredjian, "Simulation of Startup Sequence of an Offshore Wind Farm With MMC-HVDC Grid Connection," *IEEE Transactions on Power Delivery*, vol. 32, no. 2, pp. 638–646, Apr. 2017.

[21] O. Saborío-Romano, A. Bidadfar, J. N. Sakamuri, Ö. Göksu, and N. A. Cutululis, "Novel Energisation Method for Offshore Wind Farms Connected to HVdc via Diode Rectifiers," in *Proceedings of the 45th IEEE IES Annual Conference (IECON 2019)*, Lisbon, Portugal, 14th–17th Oct. 2019.

[22] E. Muljadi, S. Pasupulati, A. Ellis, and D. Kosterov, "Method of Equivalencing for a Large Wind Power Plant with Multiple Turbine Representation," in *Proceedings of the IEEE PES 2008 General Meeting*, Pittsburgh, PA, United States, 20th–24th Jul. 2008.


**Oscar Saborío-Romano** (S'12) received the BSc (Hons) degree in Electrical Engineering from the University of Costa Rica in 2013. In 2015, he received the MSc degrees in Electrical Engineering and Wind Energy from Delft University of Technology and the Norwegian University of Science and Technology, respectively. He joined the Department of Wind Energy at the Technical University of Denmark in 2016, where he is currently pursuing a PhD. His research interests include power system control and stability, integration of renewable energy sources, modelling and control of wind power, HVdc transmission, and microgrids.

**Ali Bidadfar** (M'14) worked as a power system researcher at KTH, Stockholm, Sweden, from 2013 to 2016. He has been a PhD researcher at the Technical University of Denmark since 2016. During his PhD, he has focused on frequency support provision from offshore HVdc grids. In August 2019, he joined Ørsted, Copenhagen, Denmark, as a power system engineer. His research interests include HVdc control and operation, offshore wind generation and transmission technologies, control and stability of power systems.

**Jayachandra N. Sakamuri** received the MTech degree in Electrical Engineering from the Indian Institute of Technology in 2009, after spending a year as an exchange student at the Technical University of Berlin, Germany, in 2008. He received the PhD degree on Coordinated Control of Wind Power Plants in Offshore HVdc Grids from DTU Wind Energy. Before the PhD, he worked for Grid System R&D, ABB on HVdc System Design for three years and also at Crompton Greaves Ltd. on HV switchgear design. His research interests include HVdc, offshore WPP integration and control, and HV switchgear design.

**Ömer Göksu** received the BSc and MSc degrees in EEE from the METU, Ankara, Turkey in 2004 and 2008, respectively, and was employed in Aselsan Inc. from 2004 to 2009. He obtained his PhD degree from the Department of Energy Technology, Aalborg University, Denmark, in 2012, under the Vestas Power Programme. In 2013, he was a research associate at the University of Manchester, UK. Since 2013 he is a researcher at the Department of Wind Energy at the Technical University of Denmark. His research is focused on ac and HVdc connected wind turbine and wind power plant control and modelling, and integration of power electronics to power systems.

**Nicolaos A. Cutululis** (SM'18) received the MSc and PhD degrees, both in Automatic Control, in 1998 and 2005, respectively. Currently, he is a professor at the Department of Wind Energy, Technical University of Denmark. His main research interests are integration of wind power, with a special focus on offshore wind power, and grids.